ResearchGate

See discussions, stats, and author profiles for this publication at: https://www.researchgate.net/publication/268881712

# Preparation of Multi coloured Different sized Fluorescent Gold Clusters from Blue to NIR, Structural Analysis of the Blue Emitting Au7 Cluster and Cell-Imaging by the NIR Gold Clus…

**Article** *in* Nanoscale · November 2014

DOI: 10.1039/C4NR04338C

CITATIONS
43

READS
618

**7 authors**, including:

Arindam Banerjee
Indian Association for the Cultivation of Science
**166** PUBLICATIONS **7,045** CITATIONS
SEE PROFILE

Abhishek Baral
University of Strasbourg
**14** PUBLICATIONS **733** CITATIONS
SEE PROFILE

Rameswar Bhattacharjee
University of Delaware
**27** PUBLICATIONS **669** CITATIONS
SEE PROFILE

Batakrishna Jana
Indian Institute of Chemical Biology
**33** PUBLICATIONS **592** CITATIONS
SEE PROFILE

**Some of the authors of this publication are also working on these related projects:**



self assembly and catalysis View project



Supramolecular Gels View project

All content following this page was uploaded by Abhishek Baral on 06 June 2015.

The user has requested enhancement of the downloaded file.

Published on 28 November 2014. Downloaded by Indian Association for the Cultivation of Science on 06/06/2015 07:02:56.

Nanoscale

PAPER

View Article Online
View Journal | View Issue

Cite this: *Nanoscale*, 2015, **7**, 1912

# Preparation of multi-coloured different sized fluorescent gold clusters from blue to NIR, structural analysis of the blue emitting $Au_7$ cluster, and cell-imaging by the NIR gold cluster†

Subhasish Roy,‡[a] Abhishek Baral,‡[a] Rameswar Bhattacharjee,[b] Batakrishna Jana,[c] Ayan Datta,[b] Surajit Ghosh[c] and Arindam Banerjee*[a]

Received 30th July 2014,
Accepted 24th November 2014

DOI: 10.1039/c4nr04338c

www.rsc.org/nanoscale

Blue, green, orange-red, red and NIR emitting gold quantum clusters have been prepared in aqueous media by using a bioactive peptide glutathione (reduced) at physiological pH. Matrix-assisted laser desorption ionization-time-of-flight mass spectrometry (MALDI-TOF MS) analyses show that the core structure sizes of the five different gold clusters are $Au_7$ (blue), $Au_{16}$ (green), $Au_{19}$ (orange-red), $Au_{21}$ (red) and $Au_{22}$ (NIR). The photo-stability and pH-stability of these quantum clusters have been measured, and these are photo-stable against continuous UV irradiation for a few hours. They also exhibit moderate to good pH-stability within the pH range of 5–12.5. A computational study reveals the organisation of gold atoms in the thiolate-protected blue quantum cluster and its several structural parameters, including the mode of interaction of ligand molecules with Au atoms in the $Au_7$ cluster. Interestingly, it has been found that NIR emitting gold quantum cluster can easily be internalized into the adenocarcinomic human alveolar basal epithelial cell line (A549 cell line). Moreover, a MTT assay indicates that our NIR emitting gold quantum cluster show very low cytotoxicity to A549 cancer cells.

## Introduction

The design and synthesis of new nanomaterials with interesting functional properties has remained at the cutting-edge of scientific research for several decades. Among these nanomaterials, noble metal quantum clusters[1–22] with fascinating fluorescence properties are important. Ultra-small noble metal quantum clusters[10–22] with less number of metal atoms possess a missing link between single metal atoms and relatively large-sized nanocrystals. These quantum clusters have very small particle sizes (<2 nm), and exhibit discrete and size-tunable electronic transitions. They show unique molecule-like properties, such as quantized charging and luminescence.[1–9] Interestingly, these quantum clusters exhibit notable luminescence properties with better photo-stability and lower toxicity than those of organic fluorophores and semiconducting nanocrystals.[10–22] The small size of these noble metal quantum clusters with very low toxicity and the lack of blinking properties compared with semiconducting nanocrystals makes them attractive candidates for biological imaging,[23–26] chemical sensing[27,28] and other purposes.[29] Gold quantum clusters are commonly composed of a gold core surrounded by some stabilizing ligands.

Several synthetic routes have been applied for the synthesis of fluorescent gold quantum clusters including (a) template-assisted synthesis inside the matrix of folded proteins,[30] dendrimers[31] and cyclodextrins,[32] (b) core-etching of metallic nanoparticles or some other large core size noble metal quantum clusters to few-atom quantum clusters,[33] (c) chemical reduction of $Au^{III}$ ions using different reducing agents in the presence of definite stabilizing/capping agents[34–36] and (d) conversion of an as-synthesized quantum cluster into a larger size quantum cluster by ligand exchange with thiol-terminated ligands.[37] For designing and synthesis of quantum clusters, the colloidal synthetic route has remained unique and successful to date. However, the traditional mechanistic approach for the preparation of gold quantum clusters using solution phase methodology is much more demanding as the size of the quantum clusters can only be tuned by using this procedure.

[a]*Department of Biological Chemistry, Indian Association for the Cultivation of Science, Jadavpur, Kolkata 700 032, India. E-mail: bcab@iacs.res.in*
[b]*Department of Spectroscopy, Indian Association for the Cultivation of Science, Jadavpur, Kolkata 700032, India*
[c]*Chemistry Division, CSIR-Indian Institute of Chemical Biology, 4, Raja S. C. Mullick Road, Jadavpur, Kolkata 700032, India*

†Electronic supplementary information (ESI) available: material, instrumentation, cellular uptake studies, cytotoxicity studies, synthesis of gold clusters, UV-Vis, fluorescence, plots, reaction details in tabulated form, ESI videos. See DOI: 10.1039/c4nr04338c

‡These two authors contributed equally.



This journal is © The Royal Society of Chemistry 2015

Published on 28 November 2014. Downloaded by Indian Association for the Cultivation of Science on 06/06/2015 07:02:56.

For the synthesis of gold quantum clusters, the bottom-up approach has been applied by using the complexation of a gold salt precursor with a suitable capping ligand followed by chemical, sonochemical or microwave reduction.[38–40] For the synthesis of gold quantum clusters, commonly-used ligands include DNA,[41,42] proteins,[6,43] peptides,[44] dendrimers,[45] thiol-containing molecules[9,46] and polymers.[47] The suitable choice of ligands, reducing agents and reaction conditions are important factors for the synthesis of gold quantum clusters. To the best of our knowledge, there are no reports on the synthesis of tuneable fluorescence emissive bioactive peptide-stabilized gold quantum clusters in water at physiological pH (7.46). Keeping this in mind, a peptide with free amino, carboxylic acid and thiol groups are the best candidates for the preparation of gold quantum clusters in an aqueous medium. Though there are numerous studies on gold quantum cluster formation, only a few studies have been aimed at tuning the fluorescence emission of gold quantum clusters.[15] Hence, there is a prime need to develop different colour emitting gold quantum clusters of varying sizes in water. It is also interesting to look for a simple procedure to make different gold quantum clusters that which emit from blue to NIR. However, the direct synthesis of tuneable emission gold quantum clusters from blue to NIR in an aqueous medium by using a bioactive peptide is yet to be explored.

Apart from the synthesis of different sized gold quantum clusters, determination of the spatial orientation of gold atoms within the cluster continues to be a fascinating topic to explore, and this has been reviewed in the literature.[48–50] Several groups have investigated the structure of thiolate-protected gold quantum clusters through single crystal X-ray crystallography[51–53] and computational studies.[54,55] Structural details on phosphine-stabilized gold clusters have also been reported previously.[56,57] Although there are reports of thiolate-protected $Au_{36}$, $Au_{25}$ and $Au_{15}$ clusters, there are no earlier examples regarding the structural investigation of thiolate-protected very small-sized clusters such as $Au_7$ clusters. Therefore, it will be interesting to decipher the organisation of gold atoms with interacting ligands inside the blue emitting $Au_7$ cluster.

In this study, we have demonstrated a new synthetic procedure for the development of a series of different fluorescent blue to NIR emissive gold quantum clusters stabilized by a bioactive glutathione tripeptide (reduced) in a phosphate buffer of physiological pH (7.46) using different reducing agents and reaction conditions. We have distinguished five different colour emissive gold quantum clusters, including blue, green, orange-red, red and NIR, with moderate quantum yields, remarkable colloidal stability and long excited state life times. These gold quantum clusters are quite stable towards pH and UV light irradiation for a few hours. These tuneable, emissive gold clusters have been characterized as $Au_7$, $Au_{16}$, $Au_{19}$, $Au_{21}$ and $Au_{22}$ using MALDI-TOF MS. A structural organisation of the Au atoms and ligands in the blue emitting $Au_7$ cluster has been performed by using computational (density functional theory) and Raman spectroscopic studies. Moreover, the NIR emitting gold quantum cluster has been successfully utilized for live cancer cell imaging.

## Experimental section

Detailed experimental procedures for the synthesis of the quantum clusters are given in the ESI.†

## Results and discussion

### UV-visible spectroscopic studies

According to the spherical Jellium model, smaller and larger AuQCs emit at shorter and longer wavelengths respectively.[11] Images of these as-synthesized gold quantum clusters in glass vials under UV light are shown in Fig. 1.

The UV-Vis characteristics of the gold quantum clusters and their formation kinetics over time are illustrated in Fig. S1.† During the synthesis of the gold quantum clusters (QC1) there was initially an absorption band at 470 nm (Fig. S1a†). However, this band disappeared within a few hours with the observation of two peaks at 354 nm and 370 nm (Fig. S1a†). This suggests that the size of the gold cluster is very small.[14] Fig. S2a–e† show cluster formation and corresponding changes in colour (under visible light and UV light separately) with respect to time. No absorption band was observed in the visible region due to the formation of small-sized quantum clusters with the progress of the reaction (Fig. S1a†). Fig. S1b† shows the time-dependent formation of QC2. QC2 was prepared by using tri-sodium citrate as a reducing agent in aqueous medium at a temperature of 140 °C. Initially, no absorption peak was observed in the UV-Vis region. However, with the progress of time a new peak at 335 nm started to appear. This indicates that it is a gold-containing cluster a few atoms in size, and so the cluster size is small. The time-dependent colour change during the formation of QC2 under both visible and UV light is shown in the Fig. S2b.† It takes about 16 hours to complete the reduction and the concomitant formation of the gold cluster, as tri-sodium citrate is a mild reducing agent. The formation of QC3 and their time-dependent colour changes under visible light and UV light are shown in Fig. S1c and S2c† respectively. The

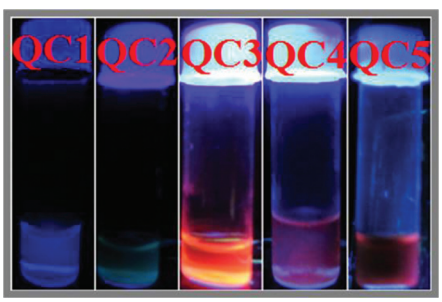


**Fig. 1** Camera images of the gold quantum clusters under UV light irradiation in 365 nm wavelength.

Published on 28 November 2014. Downloaded by Indian Association for the Cultivation of Science on 06/06/2015 07:02:56.

red emitting QC4 was synthesized by using sodium borohydride as a reducing agent at low temperature (0 °C). During the progress of the reaction, the UV-Vis changes and colour changes under visible light and under UV light were monitored (Fig. S1d and S2d†). Initially, just after the addition of sodium borohydride, there was no absorption peak in the UV-Vis region. However, after the progress of the reaction, a small new peak at 550 nm was observed. The cluster size is relatively large due to the presence of a small peak in the visible region.[32] The time-dependent UV-Vis changes of QC5 are shown in Fig. S1e,† and Fig. S2e† illustrates the gradual colour change during the formation of QC5. Initially, there was no peak in the UV-Vis region. However, during the progress of the reaction two small peaks at 463 nm and 644 nm were observed. After the completion of the reaction a small peak at 462 nm was observed, indicating the formation of relatively large-sized gold quantum clusters.[32]

## Fluorescence studies

Fluorescence emission from the blue to NIR region obtained from Au or Ag clusters is dependent on the number of atoms present within the ligand-capped cluster's core.[15] The preparation of different sized gold quantum clusters with different colour (fluorescence) emission (blue to NIR) at physiological pH in aqueous media has received tremendous research interest in recent years due to the various applications of these clusters. In this study, we have made five different colour emissive gold quantum clusters with tuneable emission. The formation kinetics of these gold quantum clusters is shown in the Fig. 2. Initially, for all gold quantum clusters, just after the addition of a reducing agent into the corresponding reaction mixture there is no fluorescence emission. After completion of the reaction, all gold quantum clusters showed bright fluorescence emission under UV light irradiation at 365 nm, as shown in Fig. 1. The QC1 gold quantum cluster shows fluorescence emission (FL) and fluorescence excitation (FLE) maxima at

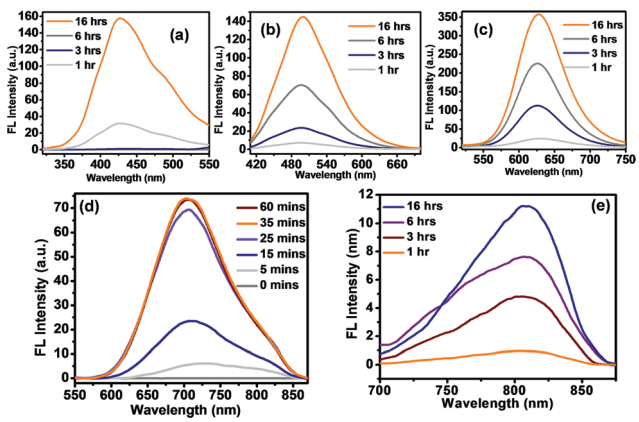


Fig. 2 Time-dependent fluorescence spectra showing the formation kinetics of the different quantum clusters (a) QC1, (b) QC2, (c) QC3, (d) QC4 and (e) QC5 measured at fluorescence excitations of 355 nm, 358 nm, 448 nm, 576 nm and 590 nm respectively.

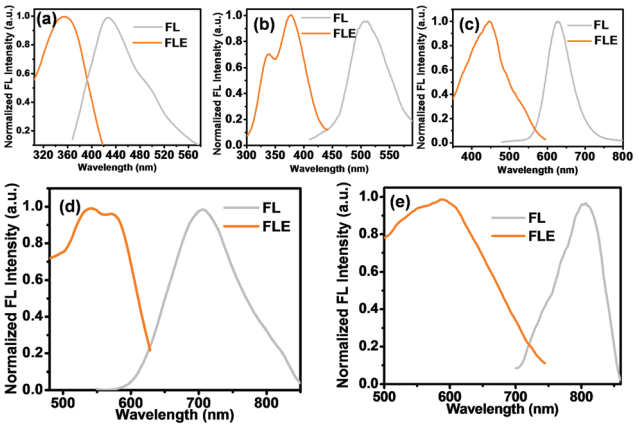


Fig. 3 Fluorescence emission (FL) and excitation (FLE) spectra of (a) QC1, (b) QC2, (c) QC3, (d) QC4 and (e) QC5 with fluorescence emissions of 426 nm (blue), 507 nm (green), 628 nm (orange-red), 705 nm (red) and 805 nm (NIR) respectively.

426 nm and 355 nm respectively. The FL and FLE spectra of this blue emitting gold quantum cluster are shown in Fig. 3a. This quantum cluster shows blue light emission under UV light irradiation (Fig. S2a (ii)†).

The as-synthesized gold quantum cluster QC2 shows a fluorescence excitation maximum at 378 nm, with a small peak at 338 nm and an emission maximum at 507 nm (Fig. 3b). This QC2 gold quantum cluster shows green fluorescence emission under UV light irradiation (Fig. S2b (ii)†). However, the QC3 gold quantum cluster shows a fluorescence excitation (FLE) peak at 448 nm and a fluorescence emission (FL) peak at 628 nm (Fig. 3c). This QC3 gold quantum cluster possesses another minor peak at 503 nm (with a much lower intensity than the major peak) upon excitation at 448 nm, with a major peak centered at 628 nm (Fig. S3†). This QC3 gold cluster exhibits a very intense orange-red colour under the exposure of UV light (365 nm) (Fig. S2c (ii)†). A fluorescence emission peak at 705 nm and excitation peaks at 540 nm and 576 nm have been observed for the QC4 gold quantum cluster (Fig. 3d). This gold quantum cluster shows a bright red emission under UV light irradiation at 365 nm (Fig. S2d (ii)†). It is interesting to note that the successfully synthesized NIR emitting gold cluster (QC5) has an emission maximum of 805 nm and fluorescence excitation at 590 nm (Fig. 3e). This QC5 gold quantum cluster exhibits a red emission under UV light irradiation (Fig. S2e (ii)†). There is a previous report regarding the synthesis of protein-stabilized blue (emission at 402 nm with a shoulder at 480 nm), green (510 nm) and red (670 nm) gold quantum clusters by using a pH variance.[15] However, in this study we have developed a new procedure for making five different gold quantum clusters, namely blue (426 nm), green (507 nm), orange-red (628 nm), red (705 nm) and NIR (805 nm), at physiological pH (7.46).

We have estimated the quantum yields of these gold quantum clusters with respect to some reference dyes. The quantum yield of QC1, QC2, QC3, QC4 and QC5 are 0.38% with respect to quinine sulphate, 0.12% with respect to atto

 This journal is © The Royal Society of Chemistry 2015

Published on 28 November 2014. Downloaded by Indian Association for the Cultivation of Science on 06/06/2015 07:02:56.

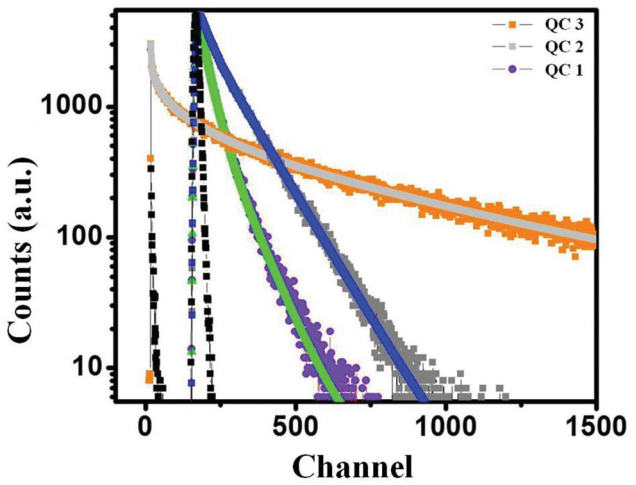


Fig. 4 Fluorescence excited state decay profiles of the QC1, QC2 and QC3 gold quantum clusters with respect to their emissions at 433 nm, 507 nm and 628 nm respectively. The estimated average fluorescence decay times are 1.06 ns, 1.32 ns and 245.10 ns for QC1, QC2 and QC3 respectively.

465, 1.2% with respect to atto 520, 0.14% with respect to rhodamine B and 0.045% with respect to rhodamine B respectively. The maximum quantum yield among these gold quantum clusters is obtained for orange-red emitting QC3 and the minimum quantum yield for NIR emitting QC5.

The fluorescence excited state life times of some of these gold quantum clusters have also been estimated, and the decay profile of these quantum clusters are shown in the Fig. 4. Average fluorescence decay times of these quantum clusters QC1, QC2 and QC3 have been estimated to be 1.06 ns with respect to its emission maximum (433 nm), 1.32 ns with respect to its emission maximum (507 nm) and 245.10 ns with respect to the 628 nm emission peak respectively.

We also checked the fluorescence emission of these gold quantum clusters at different fluorescence excitation wavelengths to check the reality of these emission peaks. The re-emission profiles at different excitation wavelengths are shown in Fig. S4.† This indicates that the fluorescence emissions of these quantum clusters are real in nature, and different emission profiles shown by those fluorescent gold quantum clusters are due to inter-band transitions from the d orbital of gold to the sp orbital of gold for lower wavelength emissive gold clusters and intra-band transitions in sp orbitals of gold for higher wavelength emissive gold quantum clusters.[58]

### pH and photo-stability

The pH stability and photo-stability of these gold quantum clusters were also examined by using fluorescence spectroscopy, and is shown in Fig. S5.† The QC1 and QC2 clusters are very much stable towards pH values ranging from 5 to 12.5 (Fig. S5a and S5b†). However, at lower pH the stability of the QC1 and QC2 gold clusters is slightly less than at moderate to high pH. The pH stability of QC3, QC4 and QC5 is very good within the range of pH 5 to 10. However, at lower and higher pH the stability (Fig. S5c–e†) of QC3, QC4 and QC5 is not so good. It is clear from the pH stability profiles of these gold quantum clusters that the lower size clusters are very stable at moderate to high pH. However, the larger size clusters are only stable at moderate pH and not in higher or lower pH. The photo-stability of these gold quantum clusters has been checked under 3 hours of UV light irradiation, and is shown in Fig. S6.† The stability of all of these quantum clusters towards UV light is diminished after 3 hours irradiation except for the QC5 cluster. Thus, the photo-stability of the QC5 gold quantum cluster is much higher as it shows very good stability even after 3 hours of UV-light irradiation. This may be due to the fact that the amount of energy supplied by the 365 nm UV light is not enough to break this cluster.

### MALDI-TOF MS analysis

The exact sizes of these gold quantum clusters or, in other words, the exact number of atoms present in the core of these clusters, have been determined by positive mode MALDI-TOF MS analysis by using 2,5-dihydroxybenzoic acid as a matrix. The MALDI-TOF MS analysis profiles of these gold quantum clusters are provided in Fig. 5. We have performed this experiment several times for the determination of the number of atoms present in the core of these different size gold quantum clusters, and these clusters are MALDI-TOF silent beyond $m/z$ 2000 at lower matrix to cluster ratios. However, at higher matrix to cluster ratios, the stability of these clusters is much improved. At a 1 : 20 cluster to matrix ratio we have achieved the stability and flying factor to optimize the conditions, and under these conditions a good distribution and reproducible

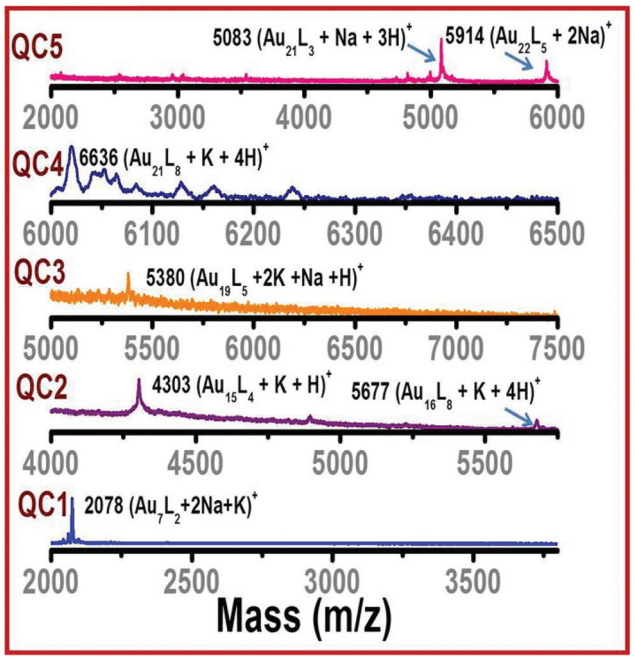


Fig. 5 MALDI-TOF MS analyses of various gold quantum clusters, using 2, 5-dihydroxybenzoic acid as a matrix.

Published on 28 November 2014. Downloaded by Indian Association for the Cultivation of Science on 06/06/2015 07:02:56.

*m*/*z* values for all gold quantum clusters (from $Au_7$ to $Au_{22}$) were obtained.

Here, the peak at *m*/*z* value of 2078 for QC1 corresponds to the $(Au_7L_2 + 2Na + K)^+$ ion, while ions that can be assigned for QC2 are $(Au_{15}L_4 + K + H)^+$ and $(Au_{16}L_8 + K + 4H)^+$, expressed as *m*/*z* peaks at 4303 and 5677 respectively. Similarly, the corresponding ion for QC3 at a *m*/*z* value of 5380 is $(Au_{19}L_5 + 2K + Na + H)^+$. The peak at 6636 for QC4 comes from the $(Au_{21}L_8 + K + 4H)^+$ ion, while the two peaks at 5083 and 5914 for QC5 correspond to the $(Au_{21}L_3 + Na + 3H)^+$ and $(Au_{22}L_5 + 2Na)^+$ ions respectively. In this study, peaks at higher *m*/*z* values are considered as core peaks, and peaks with lower *m*/*z* values correspond to fragmented species.[59] Thus, the quantum clusters QC1, QC2, QC3, QC4 and QC5 are composed of $Au_7$, $Au_{16}$, $Au_{19}$, $Au_{21}$ and $Au_{22}$ core structures respectively.

### FTIR study

To gain insight into the surface chemistry of the gold cluster, FTIR experiments was carried out with the dried blue cluster (QC1), and it was compared with the FTIR spectrum of the glutathione (reduced) ligand. The characteristic peak for the –SH (thiol) group at 2530 $cm^{-1}$ (Fig. S8†) in glutathione was absent in the case of the blue emitting gold cluster. This indicates the participation of the thiol group in stabilizing the Au atoms within the gold cluster.

### TEM study

Transmission electron microscopy (TEM) studies were carried out with the NIR ($Au_{22}$) gold cluster (Fig. 6), and it was apparent that most of these spherical shaped particles lie within the range of 1.4–1.8 nm. However, there are also some nanoparticles with diameters of more than 2 nm. These can arise due to the aggregation of smaller particles. This can commonly occur in organic ligand-capped small particles when TEM imaging is carried out under a strong electron beam operating at a high acceleration voltage of 200 keV.[60] TEM imaging of the smaller clusters was not carried out. This is because it is very difficult to confirm the size tuning in such a small range, as the difference in size between the blue and NIR clusters is in the order of a few tenths of a nanometer.

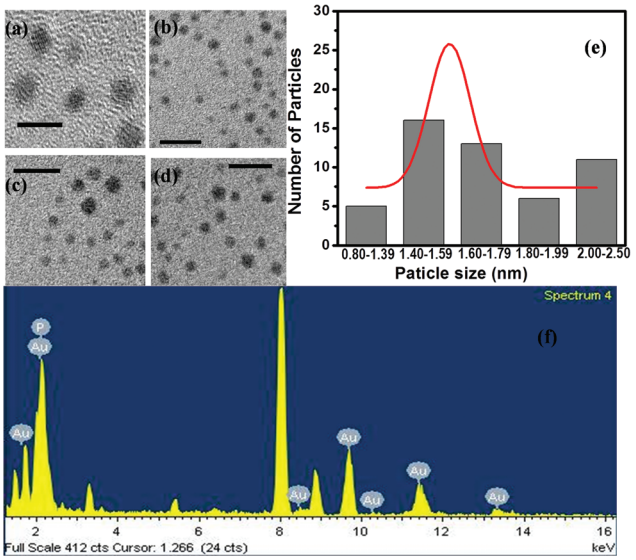


Fig. 6 (a–d) Field-emission gun transmission electron microscopy (FEG-TEM) images of the NIR gold cluster [scale bar: (a) 5 nm, (b)–(d) 10 nm], (e) particle size distribution obtained from the TEM images, and (f) (b) energy dispersive X-ray (EDX) studies confirming the presence of gold particles.

### XPS study

The valence of Au cores within the gold clusters can be determined from the X-ray photo electron spectroscopic (XPS) studies of these clusters. XPS analysis of the NIR cluster (Fig. S9†) show binding energy peaks at 87.46 eV and 83.78 eV for $4f_{5/2}$ and $4f_{7/2}$ respectively. Deconvolution of the $4f_{7/2}$ peak suggests peaks at 84.28 eV (orange line) and 83.64 eV (green line) corresponding to Au(I) and Au(0) respectively.[61]

### Detailed structural investigation of the $Au_7$ blue cluster using Raman and computational studies

An attempt has been made to make a tentative model for the blue emitting $Au_7$ structure on the basis of Raman spectral analysis of this cluster and computational studies. Fig. S10† reveals that the sulphur atom of the peptide ligand (glutathione) interacts with the gold atom, as evidenced by the presence of a Raman stretching frequency of the Au–S bond at 234 $cm^{-1}$.[62,63] In order to investigate the bonding nature between ligands and gold atoms in the cluster, we have performed a Raman spectroscopic experiment of the gold cluster along with its deuterated analogue. This will explain whether SH or $S^-$ interacts with gold atoms. Interestingly, Raman bands at 234 $cm^{-1}$ for Au–S stretching and 679 $cm^{-1}$ for C–S stretching vibrations in the ligand were observed for both the native cluster and its deuterated analogue.[64] Thus, no shift on H/D exchange in Raman spectral analysis suggests interaction of the thiolate ($S^-$) group (not the thiol) with the gold atoms in the $Au_7$ cluster.

For understanding the molecular mechanism of the interaction of glutathionate molecules with the Au clusters, the structure of the smallest cluster, $Au_7$(glutathionate)$_2$, was investigated *via* density functional theory (DFT). Considering the formidable number of atoms in even the smallest of the clusters in the series, we performed quantum mechanics and molecular mechanics (QM/MM)-based hybrid calculations[65] on $Au_7$(glutathionate)$_2$. The chemically relevant 7 Au atoms, the anchoring S atoms and the $-CH_2-$ groups connected to the S atoms of the glutathionate molecules were included in the QM region, and the other atoms of the glutathionate groups were considered at the MM level. For the QM region, the hybrid meta GGA functional, namely the M06-2X functional, was utilized.[66] A relativistic effective core potential (ECP), LANL2TZ, was used for the Au atoms,[67] while the Pople's split basis, 6-31 + G(d,p), was used for the anchoring S atoms, C atoms and H atoms in the QM region. The universal force field (UFF) was used for the MM calculations.[68] All of these cal-

 This journal is © The Royal Society of Chemistry 2015

Published on 28 November 2014. Downloaded by Indian Association for the Cultivation of Science on 06/06/2015 07:02:56.

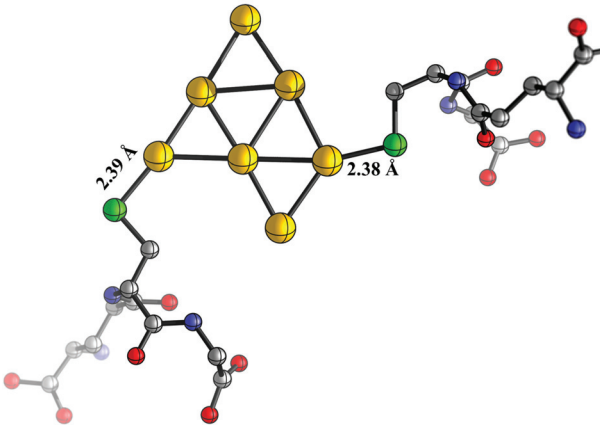


Fig. 7 Structure of the optimized $Au_7(glutathionate)_2$ cluster at M06-2X/LANL2TZ:Au, 6-31 + G(d, p): S, C, H; UFF for other atoms of glutathionate (colour notations for atoms: Au = gold, S = green, C = grey, N = blue and O = red).

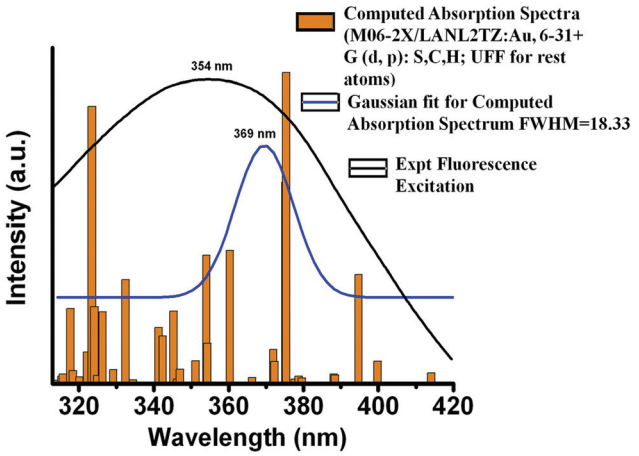


Fig. 8 Experimental fluorescence excitation spectrum and the computed fluorescence excitation spectrum.

culations were performed using the Gaussian 09 suite of programs.[69] The structure of the optimized $Au_7(glutathionate)_2$ cluster is shown in Fig. 7. The structure of the $Au_7$ core remains planar and resembles the structure of the naked $Au_7$ cluster (with $C_s$ symmetry), as computed previously by several groups.[70] The Au–S bond lengths are 2.39 Å and 2.38 Å, which are significantly lower than the sum of their van der Waals radii ($r_{Au}$ = 1.66 Å; $r_S$ = 1.80 Å),[71] suggesting a bonding interaction between the metal atoms and the thiolate anchors. An analysis of the Mulliken charge density shows substantial charge delocalization between the $S^-$ atoms and the $Au_7$ cluster, with the two anchoring sulphur atoms possessing small localized charges $q = -0.19e$ and $-0.16e$, and the rest of the negative charge density being smeared out across the seven Au atoms of the cluster.

Time-dependent DFT calculations were performed for the geometry-optimized structure of $Au_7(glutathionate)_2$ at the same level of theory. The computed optical transition at 375.4 nm involving excitation from the HOMO to LUMO levels (oscillator strength, $f = 0.16$) is in excellent agreement with the peak associated with the experimental fluorescence excitation ($\lambda_{max}$ = 354 nm). Fig. 8 shows the experimental fluorescence excitation spectrum along with the computed fluorescence excitation spectrum.

In order to understand the nature of molecular vibrations in the $Au_7(glutathionate)_2$ cluster, additional harmonic frequency calculations were performed, which were used to estimate the non-resonance Raman vibrations. The experimental non-resonance Raman excitations were performed using a 676.4 nm red $Kr^+$ laser, and we critically analyzed the Raman bands in this region. The experimentally observed intense Raman band of 679 $cm^{-1}$ is assigned to the C–S stretching mode based on our computations ($\nu(C–S)_{computed}$ = 689 $cm^{-1}$; Raman scattering activity = 3.96 $Å^4$ $amu^{-1}$), and the experimental band at 234 $cm^{-1}$ is assigned to the Au–S stretching mode based on our calculations ($\nu(Au–S)_{computed}$ = 260 $cm^{-1}$; Raman scattering activity = 3.10 $Å^4$ $amu^{-1}$). Fig. S10† shows the observed and the computed Raman spectra for the $Au_7(glutathionate)_2$ cluster. Animations of the Raman active C–S vibrational normal mode and the Au–S vibrational normal mode are provided as ESI video 1 and 2† respectively. Deuterium exchange in the complex leads to no change in the observed Raman spectrum, thereby excluding the possibility of existence of the protonated glutathione on the surface of the Au clusters.

## Cell imaging

After the synthesis and characterization of different new fluorescent gold quantum clusters, we became interested in whether these fluorescent gold quantum clusters can be used as a fluorescent probe for delivering different bio-molecules such as drugs, proteins *etc.* into cancer cells. For this we checked the cell imaging properties of these new gold quantum clusters using the adenocarcinomic human alveolar basal epithelial cell line (A549 cell line). A549 cells were seeded onto a cover glass bottom dish and imaged after treatment with these new gold quantum clusters. For this experiment, the concentration of the cells and QC5 were 5000 cells per confocal disk and 2 mg $mL^{-1}$ respectively, and the incubation time was fixed at 4 hours at 37 °C. Interestingly, it was found that the NIR emitting gold quantum cluster can easily internalize into the cell, as we observe strong red fluorescence signals inside the A549 cell line in the 561 nm channel (Fig. 9b). Fig. 9a shows the DIC image of the A549 cell line and Fig. 9c is the merged image. The fluorescence image of blank cells (without the treatment of AuNCs) under the same imaging conditions (Fig. S11†) proves that the fluorescence output does not result from the auto-fluorescence of cells. Moreover, we studied the cytotoxicity of this NIR emitting gold quantum cluster by MTT assay,[72,73] and it was found that our NIR emitting gold quantum cluster has very low cytotoxicy to the A549 cancer cells, as the cells have around an 80% viability upon the treatment of NIR emitting gold quantum cluster at 100 μg $mL^{-1}$ maximum concentration (Fig. 9d). From the above results, we

Published on 28 November 2014. Downloaded by Indian Association for the Cultivation of Science on 06/06/2015 07:02:56.

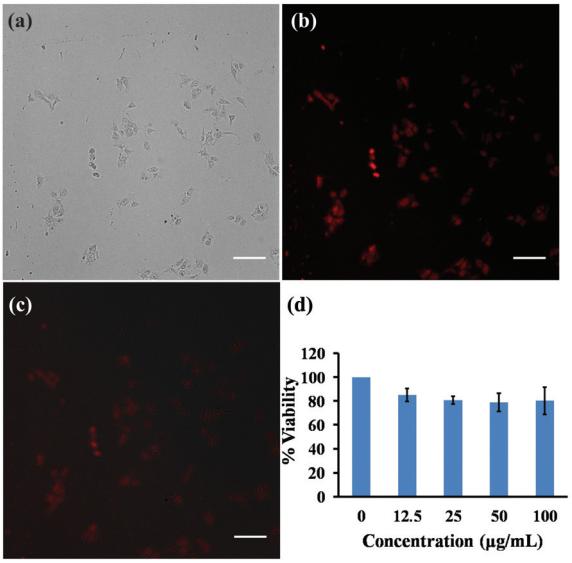


**Fig. 9** Cellular uptake of the NIR emitting gold quantum cluster in the adenocarcinomic human alveolar basal epithelial cell line (A549 cell line). (a) DIC image of the A549 cell line; (b) fluorescence image of the A549 cell line in the 561 nm channel clearly shows the uptake of NIR emitting gold quantum cluster; (c) merged image (scale bar 20 μm); (d) the cytotoxicity of the NIR emitting gold quantum cluster was assessed by MTT assay in the A549 cell line for 24 hours.

can conclude that our near infrared (NIR) gold quantum clusters can be used as fluorescent probes for cell imaging and delivering biomolecules simultaneously.

## Conclusion

A novel method has been developed for making five different gold quantum clusters with varying sizes emitting from the blue to NIR region by using a bioactive peptide glutathione at physiological pH conditions. MALDI-TOF MS analyses clearly indicate the formation of $Au_7$ (for blue emission), $Au_{16}$ (for green emission), $Au_{19}$ (for orange-red emission), $Au_{21}$ (for red emission) and $Au_{22}$ (for NIR emission) clusters. These gold quantum clusters show good pH stability within the pH range of 5.0 to 9.0 and photo-stability against continuous UV radiation for a few hours. Raman spectral analysis and computational studies reveal a tentative model structure of the blue emitting $Au_7$ cluster, showing the interacting gold atoms with the corresponding ligands in the cluster. Interestingly, the NIR emitting gold cluster has been easily internalized into the adenocarcinomic human alveolar basal epithelial cell line (A549 cell line), and the MTT assay shows that this NIR emitting gold quantum cluster has very low cytotoxicity to the A549 cancer cells as the cells have a viability of around 80% upon the treatment of NIR emitting gold quantum clusters at a maximum concentration of 100 μg $mL^{-1}$. The tuning of the fluorescence emission from blue to NIR in water at physiological pH gives future promise for synthesizing different colour tuneable gold clusters for various biotechnological and biomedical applications.

## Acknowledgements

A. B., R. B. and B. J. gratefully acknowledge CSIR, New Delhi (India) for financial assistance. S.G. acknowledges DST, India for the Ramanujan fellowship and CSIR-IICB network project (BSC0113) for financial support. A. D. thanks DST and INSA for partial funding. We acknowledge the Department of Science and Technology, India grant DST/SR/IC-35-2009 for the Raman spectroscopic instrument.

## Notes and references

1 R. Jin, *Nanoscale*, 2010, **2**, 343–362.
2 I. Díez and R. H. A. Ras, *Nanoscale*, 2011, **3**, 1963–1970.
3 S. M. Reilly, T. Krick and A. Dass, *J. Phys. Chem. C*, 2010, **114**, 741–745.
4 L. Shang, S. Dong and G. U. Nienhaus, *Nano Today*, 2011, **6**, 401–418.
5 T. Laaksonen, V. Ruiz, P. Liljeroth and B. M. Quinn, *Chem. Soc. Rev.*, 2008, **37**, 1836–1846.
6 J. Xie, Y. Zheng and J. Y. Ying, *J. Am. Chem. Soc.*, 2009, **131**, 888–889.
7 H. Xu and K. S. Suslick, *Adv. Mater.*, 2010, **22**, 1078–1082.
8 S. Roy and A. Banerjee, *Soft Matter*, 2011, **7**, 5300–5308.
9 B. Adhikari and A. Banerjee, *Chem. Mater.*, 2010, **22**, 4364–4371.
10 J. Zheng, J. T. Petty and R. M. Dickson, *J. Am. Chem. Soc.*, 2003, **125**, 7780–7781.
11 J. Zheng, C. Zhang and R. M. Dickson, *Phys. Rev. Lett.*, 2004, **93**, 077402.
12 L. Shang, N. Azadfar, F. Stockmar, W. Send, V. Trouillet, M. Bruns, D. Gerthsen and G. U. Nienhaus, *Small*, 2011, **7**, 2614–2620.
13 F. Aldeek, M. A. H. Muhammed, G. Palui, N. Zhan and H. Mattoussi, *ACS Nano*, 2013, **7**, 2509–2521.
14 S. Roy, G. Palui and A. Banerjee, *Nanoscale*, 2012, **4**, 2734–2740.
15 H. Kawasaki, K. Hamaguchi, I. Osaka and R. Arakawa, *Adv. Funct. Mater.*, 2011, **21**, 3508–3515.
16 C.-C. Huang, Z. Yang, K.-H. Lee and H.-T. Chang, *Angew. Chem., Int. Ed.*, 2007, **46**, 6824–6828.
17 B. Adhikari and A. Banerjee, *Chem. – Eur. J.*, 2010, **16**, 13698–13705.
18 X. Yuan, Z. Luo, Y. Yu, Q. Yao and J. Xie, *Chem. – Asian J.*, 2013, **8**, 858–871.
19 F. Aldeek, X. Ji and H. Mattoussi, *J. Phys. Chem. C*, 2013, **117**, 15429–15437.
20 Y. Kamei, Y. Shichibu and K. Konishi, *Angew. Chem., Int. Ed.*, 2011, **50**, 7442–7445.
21 S. Roy, A. Baral and A. Banerjee, *ACS Appl. Mater. Interfaces*, 2014, **6**, 4050–4056.
22 K. G. Stamplecoskie, Y.-S. Chen and P. V. Kamat, *J. Phys. Chem. C*, 2014, **118**, 1370–1376.
23 H.-H. Wang, C.-A. J. Lin, C.-H. Lee, Y.-C. Lin, Y.-M. Tseng, C.-L. Hsieh, C.-H. Chen, C.-H. Tsai, C.-T. Hsieh, J.-L. Shen,

 This journal is © The Royal Society of Chemistry 2015

Published on 28 November 2014. Downloaded by Indian Association for the Cultivation of Science on 06/06/2015 07:02:56.

W.-H. Chan, W. H. Chang and H.-I. Yeh, *ACS Nano*, 2011, **5**, 4337–4334.
24 T. Chen, Y. Hu, Y. Cen, X. Chu and Y. Lu, *J. Am. Chem. Soc.*, 2013, **135**, 11595–11602.
25 S. Choi, R. M. Dickson, J.-K. Lee and J. Yu, *Photochem. Photobiol. Sci.*, 2012, **11**, 274–278.
26 L. Yang, L. Shang and G. U. Nienhaus, *Nanoscale*, 2013, **5**, 1537–1543.
27 W.-Y. Chen, G.-Y. Lan and H.-T. Chang, *Anal. Chem.*, 2011, **83**, 9450–9455.
28 S. Choi, S. Park, K. Lee and J. Yu, *Chem. Commun.*, 2013, **49**, 10908–10910.
29 D. Schultz, S. M. Copp, N. Markešević, K. Gardner, S. S. R. Oemrawsingh, D. Bouwmeester and E. Gwinn, *ACS Nano*, 2013, **7**, 9798–9807.
30 Y. Yu, Z. Luo, C. S. Teo, Y. N. Tan and J. Xie, *Chem. Commun.*, 2013, **49**, 9740–9742.
31 Y.-C. Jao, M.-K. Chen and S.-Y. Lin, *Chem. Commun.*, 2010, **46**, 2626–2628.
32 E. S. Shibu and T. Pradeep, *Chem. Mater.*, 2011, **23**, 989–999.
33 H. Duan and S. Nie, *J. Am. Chem. Soc.*, 2007, **129**, 2412–2413.
34 Y. Negishi, Y. Takasugi, S. Sato, H. Yao, K. Kimura and T. Tsukuda, *J. Am. Chem. Soc.*, 2004, **126**, 6518–6519.
35 W. Chen and S. Chen, *Angew. Chem., Int. Ed.*, 2009, **48**, 4386–4389.
36 Y. Yu, X. Chen, Q. Yao, Y. Yu, N. Yan and J. Xie, *Chem. Mater.*, 2013, **25**, 946–952.
37 R. Balasubramanian, R. Guo, A. J. Mills and R. W. Murray, *J. Am. Chem. Soc.*, 2005, **127**, 8126–8132.
38 L. Shang, R. M. Dörlich, S. Brandholt, R. Schneider, V. Trouillet, M. Bruns, D. Gerthsen and G. U. Nienhaus, *Nanoscale*, 2011, **3**, 2009–2014.
39 H. Liu, X. Zhang, X. Wu, L. Jiang, C. Burda and J.-J. Zhu, *Chem. Commun.*, 2011, **47**, 4237–4239.
40 L. Yan, Y. Cai, B. Zheng, H. Yuan, Y. Guo, D. Xiao and M. M. F. Choi, *J. Mater. Chem.*, 2012, **22**, 1000–1005.
41 T. A. C. Kennedy, J. L. MacLean and J. Liu, *Chem. Commun.*, 2012, **48**, 6845–6847.
42 H.-C. Yeh, J. Sharma, J. J. Han, J. S. Martinez and J. H. Werner, *Nano Lett.*, 2010, **10**, 3106–3110.
43 Z. Chen, S. Qian, X. Chen, W. Gao and Y. Lin, *Analyst*, 2012, **137**, 4356–4361.
44 S. Kumar, M. D. Bolan and T. P. Bigioni, *J. Am. Chem. Soc.*, 2010, **132**, 13141–13143.
45 M. L. Tran, A. V. Zvyagin and T. Plakhotnik, *Chem. Commun.*, 2006, 2400–2401.
46 S. Knoppe, S. Michalet and T. Bürgi, *J. Phys. Chem. C*, 2013, **117**, 15354–15361.
47 N. Schaeffer, B. Tan, C. Dickinson, M. J. Rosseinsky, A. Laromaine, D. W. McComb, M. M. Stevens, Y. Wang, L. Petit, C. Barentin, D. G. Spiller, A. I. Cooper and R. Lévy, *Chem. Commun.*, 2008, 3986–3988.
48 Y. Pei and X. C. Zeng, *Nanoscale*, 2012, **4**, 4054–4072.
49 M. Walter, J. Akola, O. Lopez-Acevedo, P. D. Jadzinsky, G. Calero, C. J. Ackerson, R. L. Whetten, H. Grönbeck and H. Häkkinen, *Proc. Natl. Acad. Sci. U. S. A.*, 2008, **105**, 9157–9162.
50 H. Häkkinen, *Chem. Soc. Rev.*, 2008, **37**, 1847–1859.
51 C. Zeng, H. Qian, T. Li, G. Li, N. L. Rosi, B. Yoon, R. N. Barnett, R. L. Whetten, U. Landman and R. Jin, *Angew. Chem., Int. Ed.*, 2012, **51**, 13114–13118.
52 C. Zeng, T. Li, A. Das, N. L. Rosi and R. Jin, *J. Am. Chem. Soc.*, 2013, **135**, 10011–10013.
53 M. W. Heaven, A. Dass, P. S. White, K. M. Holt and R. W. Murray, *J. Am. Chem. Soc.*, 2008, **130**, 3754–3755.
54 D.-E. Jiang, S. H. Overbury and S. Dai, *J. Am. Chem. Soc.*, 2013, **135**, 8786–8789.
55 D.-E. Jiang, *Chem. – Eur. J.*, 2011, **17**, 12289–12293.
56 Y. Shichibu, Y. Kamei and K. Konishi, *Chem. Commun.*, 2012, **48**, 7559–7561.
57 Y. Shichibu and K. Konishi, *Inorg. Chem.*, 2013, **52**, 6570–6575.
58 M. A. H. Muhammed, S. Ramesh, S. S. Sinha, S. K. Pal and T. Pradeep, *Nano Res.*, 2008, **1**, 333–340.
59 Z. Wu, E. Lanni, W. Chen, M. E. Bier, D. Ly and R. Jin, *J. Am. Chem. Soc.*, 2009, **131**, 16672–16674.
60 D. Stellwagen, A. Weber, G. Lisa Bovenkamp, R. Jin, J. H. Bitter and C. S. S. R. Kumar, *RSC Adv.*, 2012, **2**, 2276–2283.
61 X. Tu, W. Chen and X. Guo, *Nanotechnology*, 2011, **22**, 095701.
62 G. J. Kluth, C. Carraro and R. Maboudian, *Phys. Rev. B: Condens. Matter Mater. Phys.*, 1999, **59**, R10449–R10452.
63 R. G. Nuzzo, B. R. Zegarski and L. H. Dubois, *J. Am. Chem. Soc.*, 1987, **109**, 733–740.
64 S. Bandyopadhyay and A. Dey, *Analyst*, 2014, **139**, 2118–2121.
65 T. Vreven, K. S. Byun, I. Komáromi, S. Dapprich, J. A. Montgomery Jr., K. Morokuma and M. J. Frisch, *J. Chem. Theory Comput.*, 2006, **2**, 815–826.
66 Y. Zhao and D. G. Truhlar, *Theor. Chem. Acc.*, 2008, **120**, 215–241.
67 L. E. Roy, P. J. Hay and R. L. Martin, *J. Chem. Theory Comput.*, 2008, **4**, 1029–1031.
68 A. K. Rappé, C. J. Casewit, K. S. Colwell, W. A. G. III and W. M. Skiff, *J. Am. Chem. Soc.*, 1992, **114**, 10024–10035.
69 M. J. Frisch, G. W. Trucks, H. B. Schlegel, G. E. Scuseria, M. A. Robb, J. R. Cheeseman, G. Scalmani, V. Barone, B. Mennucci, G. A. Petersson, H. Nakatsuji, M. Caricato, X. Li, H. P. Hratchian, A. F. Izmaylov, J. Bloino, G. Zheng, J. L. Sonnenberg, M. Hada, M. Ehara, K. Toyota, R. Fukuda, J. Hasegawa, M. Ishida, T. Nakajima, Y. Honda, O. Kitao, H. Nakai, T. Vreven, J. A. Montgomery Jr., J. E. Peralta F. Ogliaro, M. Bearpark, J. J. Heyd, E. Brothers, K. N. Kudin, V. N. Staroverov, R. Kobayashi, J. Normand, K. Raghavachari, A. Rendell, J. C. Burant, S. S. Iyengar, J. Tomasi, M. Cossi, N. Rega, J. M. Millam, M. Klene, J. E. Knox, J. B. Cross, V. Bakken, C. Adamo, J. Jaramillo,

Published on 28 November 2014. Downloaded by Indian Association for the Cultivation of Science on 06/06/2015 07:02:56.

R. Gomperts, R. E. Stratmann, O. Yazyev, A. J. Austin, R. Cammi, C. Pomelli, J. W. Ochterski, R. L. Martin, K. Morokuma, V. G. Zakrzewski, G. A. Voth, P. Salvador, J. J. Dannenberg, S. Dapprich, A. D. Daniels, Ö. Farkas, J. B. Foresman, J. V. Ortiz, J. Cioslowski and D. J. Fox, *Gaussian 09 (Revision D.01)*, Gaussian, Inc., Wallingford CT, 2009.

70 A. Nijamudheen and A. Datta, *J. Mol. Struct. (THEOCHEM)*, 2010, **945**, 93–96 and references therein.

71 A. Bondi, *J. Phys. Chem.*, 1964, **68**, 441–451.

72 B. Jana, G. Mondal, A. Biswas, I. Chakraborty and S. Ghosh, *RSC Adv.*, 2013, **3**, 8215–8219.

73 M. Jiang, O. Huang, X. Zhang, Z. Xie, A. Shen, H. Liu, M. Geng and K. Shen, *Molecules*, 2013, **18**, 701–720.



This journal is © The Royal Society of Chemistry 2015

View publication stats